ORIGINAL ARTICLE

Cancer Science WILEY

# DOC-2/DAB2 interactive protein destabilizes c-Myc to impair the growth and self-renewal of colon tumor-repopulating cells

Haiou Li[1,2]　│　Yunjiao Zhou[1,2]　│　Meng Wang[1,2]　│　Haizhou Wang[1,2]　│　Yangyang Zhang[1,2]　│　Ruyi Peng[1,2]　│　Ruike Zhang[1,2]　│　Meng Zhang[1,2]　│　Mengna Zhang[1,2]　│　Peishan Qiu[1,2]　│　Lan Liu[1,2]　│　Qiu Zhao[1,2] ⓘD　│　Jing Liu[1,2] ⓘD

[1]Department of Gastroenterology, Zhongnan Hospital of Wuhan University, Wuhan, China

[2]Hubei Clinical Center and Key Laboratory of Intestinal and Colorectal Diseases, Wuhan, China

**Correspondence**
Jing Liu, Department of Gastroenterology, Zhongnan Hospital of Wuhan University, No. 169 Donghu Road, Wuchang District, Wuhan 430071, China.
Email: liujing_GI@whu.edu.cn

**Funding information**
National Natural Science Foundation of China, Grant/Award Number: 82072753; Wuhan University, Grant/Award Number: 2042021kf0206; Zhongnan Hospital of Wuhan University, Grant/Award Number: znpy2019006

## Abstract

Colorectal carcinoma (CRC) remains a huge challenge in clinical treatment due to tumor metastasis and recurrence. Stem cell-like colon tumor-repopulating cells (TRCs) are a subpopulation of cancer cells with highly tumorigenic and chemotherapy resistant properties. The core transcription factor c-Myc is essential for maintaining cancer stem-like cell phenotypes, yet its roles and regulatory mechanisms remain unclear in colon TRCs. We report that elevated c-Myc protein supported formation and growth of TRC spheroids. The tumor suppressor DOC-2/DAB2 interactive protein (DAB2IP) suppressed c-Myc expression to inhibit TRC expansion and self-renewal. Particularly, DAB2IP disrupted c-Myc stability through glycogen synthase kinase 3β/protein phosphatase 2A-B56α-mediated phosphorylation and dephosphorylation cascade on c-Myc protein, leading to its eventual degradation through the ubiquitin-proteasome pathway. The expression of DAB2IP was negatively correlated with c-Myc in CRC specimens. Overall, our results improved mechanistic insight into how DAB2IP suppressed TRC growth and self-renewal.

**KEYWORDS**

c-Myc, colorectal cancer, DAB2IP, phosphorylation, tumor-repopulating cell

## 1 | INTRODUCTION

Colorectal cancer (CRC) ranks as the third most common malignancy and the second leading cause of cancer-related death worldwide.[1,2] In addition, the incidence of CRC in young and middle-aged adults has been increasing over the past two decades.[3,4] Hence, it is imperative to elucidate the molecular mechanisms underlying CRC tumorigenesis and progression for optimizing therapeutic strategies.

Cancer stem-like cells (CSCs) are a small subpopulation of tumor cells characterized by their self-renewal, heterogeneity, plasticity, tumorigenicity, and chemoresistance.[5,6] The presence of CSCs is recognized to facilitate tumor metastasis, recurrence, and treatment failure in CRC patients.[7] A deeper understanding of the biological features of CSCs or highly tumorigenic cells could provide novel insights into the pathogenesis of CRC. In previous studies, a highly tumorigenic subpopulation of cancer cells was enriched using a soft

Haiou Li, Yunjiao Zhou, and Meng Wang contributed equally to this work.

3D fibrin culture system.[8-10] These cells that exert crucial effects in tumor initiation and repopulation are functionally termed tumor-repopulating cells (TRCs).[10,11] TRCs display several typical characteristics of CSCs but are distinct from those stem-like cells that are isolated only based on conventional surface markers.[12,13]

The oncogene c-Myc is a well-known pleiotropic transcription factor that regulates the expression of numerous critical genes involved in essential biological processes.[14] It has been shown that c-Myc is linked to the self-renewal ability of colon tumor-initiating cells,[15,16] but the function roles and potential regulatory mechanism of c-Myc in TRCs remain unclear. DOC-2/DAB2 interactive protein (DAB2IP), a novel Ras-GTPase activating protein, is a tumor suppressor frequently downregulated in multiple aggressive tumors that regulates various biological processes.[17,18] It was demonstrated that loss of DAB2IP expression enhanced CSC-like phenotypes, suggesting its role in suppressing CSCs.[19-21] Our previous work showed that downregulation of DAB2IP in colon TRCs promoted colony growth in soft fibrin gels.[8] Nevertheless, the mechanisms by which DAB2IP regulates the growth and self-renewal of TRCs require further investigation.

In the present study, we explored the expression of c-Myc and its regulatory mechanisms in colon TRCs. We showed that DAB2IP destabilized c-Myc protein by facilitating its phosphorylation-dependent ubiquitination and eventual proteasomal degradation, thus limiting the growth and self-renewal of colon TRCs. This study delineated the functional importance of the DAB2IP-c-Myc axis in maintaining colon TRCs and CRC progression.

## 2 | MATERIALS AND METHODS

### 2.1 | Cell lines and cell culture

Human colon cancer cell lines (HCT116 and HT29) were sourced from the China Center for Type Culture Collection. Cells were cultured in RPMI-1640 (Gibco) supplemented with 10% FBS (Gibco) and 1% penicillin-streptomycin at 37°C in a 5% $CO_2$ incubator.

### 2.2 | Collection of clinical tissue specimens

Fifteen pairs of primary tumor tissues and their corresponding adjacent normal tissues were collected from CRC patients who signed informed consent at Zhongnan Hospital of Wuhan University. All the experimental procedures were approved by the clinical research institutional review board of the Zhongnan Hospital of Wuhan University and were carried out in accordance with the ethical guidelines of the Declaration of Helsinki.

### 2.3 | Cell culture in 3D fibrin gels

TRC culture was undertaken as previously described.[10] In brief, salmon fibrinogen (Searun Holdings Company) was dissolved in distilled water

at 4°C and diluted to 2 mg/mL with T7 buffer (pH 7.4, 50 mmol/L Tris, 150 mmol/L NaCl). The 125 μL precooled fibrinogen solution was mixed with 125 μL single-tumor cell solution (1:1) and seed into a precooled 24-well plate with 5 μL thrombin (0.1 U/μL; Searun Holdings). The cells were supplemented with 1 mL complete culture medium after incubation for 30 minutes at 37°C. After 5 days of culture, the cells were collected by sequential digestion with Dispase II (Roche) for 30 minutes at 37°C and 0.25% trypsin for 3 minutes. Tumor cells cultured in flasks were used as control. For sphere formation assay, a total of 1250 cells were seeded in fibrin gel and cultured for 5 days. The colony number was counted at 96 hours under an inverted microscope (Olympus). For colony size measurement, 50 spheroids per group were randomly photographed with a light microscope and analyzed by ImageJ software. For serial passage experiments, tumor spheriods were disaggregated into single cell suspension at the fifth day postplating and reseeded into a precooled 24-well plate to generate secondary spheroids for another 5 days. Tertiary spheroids were generated from the secondary spheres using the same process.

### 2.4 | Quantitative RT-PCR

Total cellular RNA was extracted using TRIzol reagent (Invitrogen) and reverse transcribed to cDNA using Transcript First-strand cDNA Synthesis Super Mix (Roche) according to the manufacturer's instructions. Quantitative PCR was carried out with UltraSYBR mixture (Cwbio) on Roche LightCycler 96 according to standard PCR conditions. Primer sequences are listed in Table S1.

### 2.5 | Cell transfection

Small interfering RNA oligonucleotides and the corresponding negative control were purchased from RiboBio. pcDNA3.1(+) and pcDNA3.1(+)-DAB2IP plasmids were gifted by Professor Daxing Xie of the Tongji Cancer Research Institute. Commercialized recombinant pCMV3-vector and pCMV3-MYC plasmids were chemically synthesized by Sino-Biological. The indicated siRNAs and plasmids were transfected into cells using Lipofectamine 2000 (Invitrogen) according to the manufacturer's protocol. The siRNA sequences are listed in Table S2.

### 2.6 | Immunoblotting

Immunoblotting assays were carried out as previously described[9] with the following primary Abs: DAB2IP (23582-1-AP, Proteintech), c-Myc (ab32072, Abcam), c-Myc (67447-1-Ig, Proteintech), p-c-Myc$^{S62}$ (ab185656, Abcam), p-c-Myc$^{T58}$ (ab185655, Abcam), glycogen synthase kinase 3β (GSK3β; 10044-T32, SinoBiological), p-GSK3β$^{S9}$ (#5558, CST), Bcl-2 (12789-1-AP, Proteintech), Bax (#5023, CST), B56α (ab89621, Abcam), Ubiquitin (10201-2-AP, Proteintech), Ubiquitin

(linkage-specific K48) (ab140601, Abcam), Nanog (#8822S, CST), CD44 (60224-1-Ig, Proteintech), CD133 (18470-1-AP, Proteintech), and GAPDH (60004-1-Ig, Proteintech). Secondary Abs conjugated to HRP (Servicebio) were used, followed by chemiluminescence.

## 2.7 | Cycloheximide chase assay

Cells were treated with 100 μg/mL cycloheximide (CHX; Selleck) and harvested at the indicated time points. Total protein was extracted and subjected to immunoblot analysis. Relative protein expression was measured using ImageJ software, with GAPDH used as a loading control.

## 2.8 | Immunoprecipitation

HCT116 and HT29 cells were lysed with ice-cold lysis buffer containing freshly added protease and phosphatase inhibitors. After preclearing with protein A/G-agarose beads, the cell lysates were then incubated with IgG, anti-DAB2IP, anti-c-Myc, or anti-B56α Abs overnight at 4℃ with continuous inversion and precipitated with protein A/G-agarose beads (Santa Cruz Biotechnology) for 3 hours. Immunoprecipitated beads were collected and washed three times. Immunocomplexes were eluted and subjected to immunoblot analysis with the indicated Abs. The input was 2% of cell lysates prior to immunoprecipitation.

## 2.9 | Ubiquitination assay

For ubiquitination assay, cells were treated with 10 μmol/L MG132 (MedChemExpress) for another 6 hours before harvesting, and then collected for immunoprecipitation with IgG or anti-c-Myc Ab followed by immunoblot analysis of ubiquitin.

## 2.10 | Animal models

The 6-week-old BALB/c nude mice were purchased from Beijing Vital River Laboratory Animal Technology Company. All animal experiments were carried out using standard methods and approved by the Animal Ethics Committee of Wuhan University. Control cancer cell suspensions or TRC suspensions ($1 \times 10^5$) were subcutaneously injected into each mouse (n = 6 per group). All mice were killed after 4 weeks, and the tumors were excised and weighed. Tumor tissues were fixed in paraformaldehyde, embedded in paraffin, and sectioned for subsequent immunofluorescence (IF) and immunohistochemistry (IHC) assessment.

## 2.11 | Immunofluorescence and Immunohistochemistry

For cell experiments, collected cells were fixed with 4% paraformaldehyde for 30 minutes and permeabilized with 0.2% Triton X-100

for 15 minutes at room temperature. Fixed cells were blocked in 5% BSA, probed with the primary Abs at 4℃ overnight, and stained with corresponding secondary Abs conjugated to FITC (Servicebio), CY3 (Servicebio), or Alexa Fluor 647 (Beyotime) for 2 hours and further counterstained with DAPI. IF and IHC analysis of tumor tissues were carried out as previously described[8] with primary Abs against DAB2IP (23582-1-AP, Proteintech) and c-Myc (ab32072, Abcam). IF images were captured using a confocal microscope (Leica) or a fluorescence microscope (Olympus). The IHC images were acquired under a light microscope (Olympus).

## 2.12 | Gene Set Enrichment Analysis

Gene Set Enrichment Analysis (GSEA) was carried out using GSEA software (http://www.broadinstitute.org/gsea/). The samples were divided into two groups based on the median of DAB2IP mRNA expression in the GSE39582 dataset from Gene Expression Omnibus (GEO) database.

## 2.13 | Statistical analysis

Statistical analyses were carried out using GraphPad Prism 7.0 software (GraphPad Software). Student's *t* test (two-tailed) was used for comparison between two groups. One-way ANOVA with Bonferroni adjustment was used for the multiple comparisons. Pearson correlation analysis was used to evaluate the correlation between DAB2IP and c-Myc. For survival analysis, Kaplan-Meier survival curves were plotted and analyzed by the log-rank test. The correlation between DAB2IP expression and clinicopathologic features was analyzed using Pearson's $\chi^2$ test. Results are represented as the mean ± SEM of at least three independent experiments. Statistical significance was set at $P < .05$ (*$P < .05$, **$P < .01$, ***$P < .001$).

# 3 | RESULTS

## 3.1 | Colon TRCs display self-renewal and long-term repopulating capabilities

To enrich colon TRCs, colon tumor cells were cultured in 3D fibrin gels. The TRCs grew into spheroid-like morphological shapes (Figure 1A). In contrast to adherent cells cultured in flasks, TRCs showed a compact cell body and relaxed cytoskeleton tension (Figure 1A). The stem cell markers CD133, CD44, and Nanog were increased in colon TRCs (Figures 1B,C and S1A). In addition, colon TRCs formed new spheroids for at least three successive generations, indicating their self-renewal and long-term repopulating capabilities (Figure 1D,E). The first passage to the second passage was accompanied by increased colony size, whereas the colony size of the third passage was comparable to that of the second passage (Figure 1D). The numbers of colonies were increased as the passage
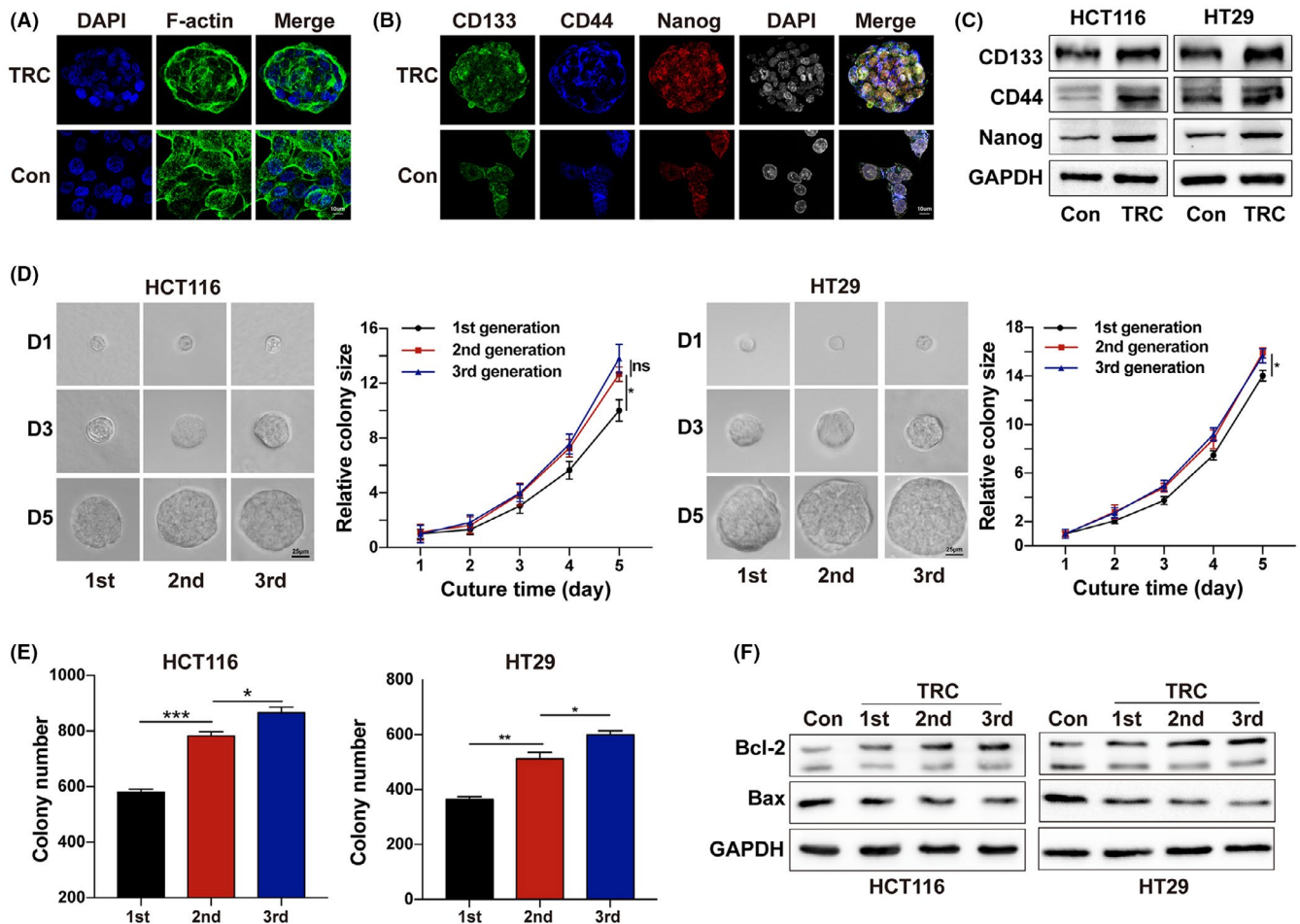
**FIGURE 1** Tumor-repopulating cells (TRCs) show self-renewal and long-term repopulating capability. A, Immunofluorescence (IF) staining of F-actin in HCT116 TRC spheroids and control monolayers with phalloidin. Scale bars, 10 μm. B, IF staining of CD133, CD44, and Nanog in HCT116 TRC spheroids and control monolayers with indicated Abs. Scale bars, 10 μm. C, Immunoblot analysis of stem markers expressed in HCT116 and HT29 TRCs, vs their control cells. D, E, Serial passage assays of HCT116 and HT29 TRCs for three successive generations. D, Left panels, Representative images of TRC spheroids. Scale bars, 25 μm. Right panels, The colony size at each passage was calculated using ImageJ software. E, Colony numbers were counted at 96 h. F, Immunoblot analysis of Bax and Bcl-2 expression in HCT116 and HT29 TRCs during serial passages. GAPDH was used as a loading control. Data are shown as the mean ± SEM (n = 3). *$P < .05$, **$P < .01$, ***$P < .001$. ns, not significant ($P > .05$). Con, control adherent cells cultured in flask

number increased (Figure 1E). In addition, the expression of proapoptosis protein Bax was decreased from first-passage spheroids, and antiapoptosis protein Bcl-2 was increased (Figure 1F). Taken together, these data suggest that TRCs mostly undergo their self-renewal and long-term repopulating capabilities.

## 3.2 | c-Myc is critical for maintaining colon TRCs

Given the widespread transcriptional activity of c-Myc and its critical roles in CSC phenotype, we explored whether c-Myc was involved in maintaining colon TRCs. The c-Myc protein was markedly increased in TRCs compared with control cells, although c-Myc mRNA levels were not significantly altered (Figures 2A and S1B). Immunohistochemical staining also showed c-Myc was upregulated in TRC xenograft tumors, in contrast with control xenograft tumors (Figure 2B). Knockdown

of c-Myc formed fewer spheroids with smaller size than the control group (Figure 2C,D). Moreover, the protein expressions of Nanog, CD133, and CD44 were attenuated in HCT116 and HT29 cells following c-Myc knockdown (Figure 2E). These observations suggest that c-Myc is required for the colon TRC maintenance.

## 3.3 | DOC-2/DAB2 interactive protein downregulates c-Myc to suppress TRC growth and self-renewal

We previously reported that downregulation of DAB2IP promoted TRC growth (Figures 3A,B and S2A,B).[8] In this study, we found that DAB2IP overexpression significantly reduced c-Myc protein levels in HCT116 and HT29 cells (Figure 3C), which was verified by IF staining (Figure 3D). In contrast, DAB2IP knockdown displayed
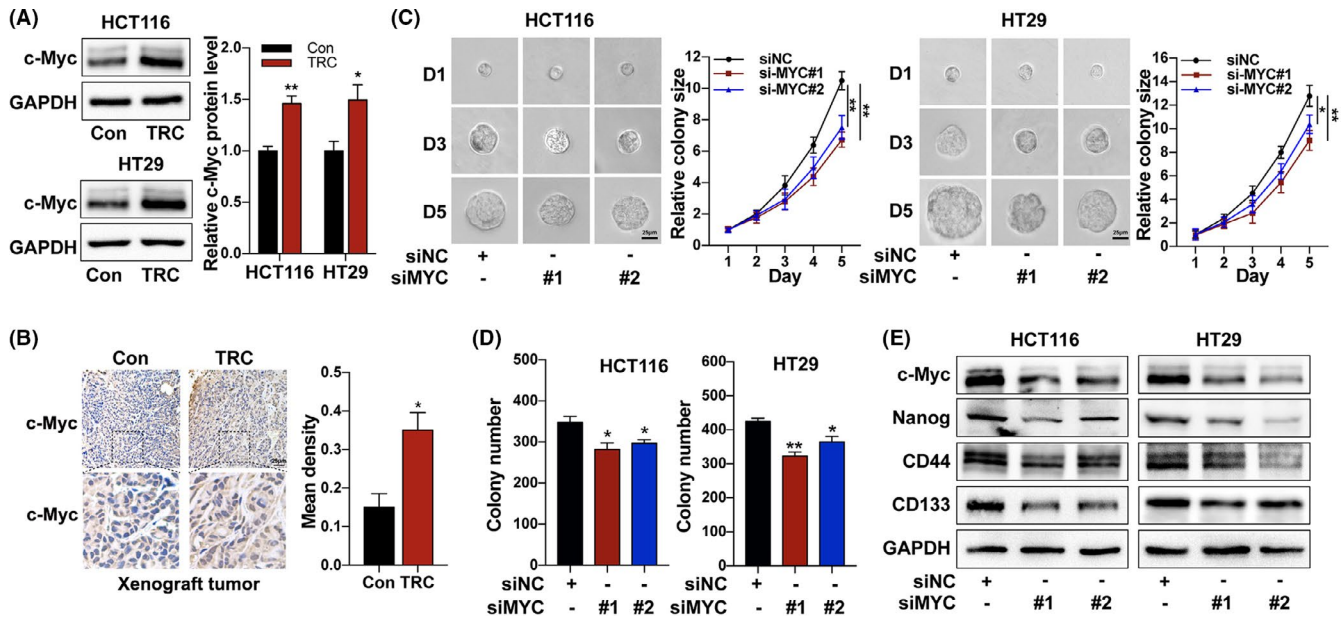
**FIGURE 2**   c-Myc is critical for maintaining colon tumor-repopulating cells (TRCs). A, Immunoblot analysis of c-Myc expression in HCT116 and HT29 TRCs, vs their control cells. Relative c-Myc protein levels were quantitated using ImageJ software. B, Immunohistochemical staining of c-Myc in the subcutaneous xenografts of HCT116 TRCs or control cells. Mean density was calculated by Image-Pro Plus 6.0. Scale bars, 25 μm. C, D, Effect of c-Myc knockdown on TRC spheroid formation and growth. C, Left panels, Representative images of TRC spheroids. Scale bars, 25 μm. Right panels, Colony size calculated by ImageJ software. D, Colony numbers were counted at 96 h. E, Immunoblot analysis of CD133, CD44, and Nanog protein levels in HCT116 and HT29 cells treated with either c-Myc siRNA or negative control siRNA (siNC). Data are shown as the mean ± SEM (n = 3). *$P < .05$, **$P < .01$, ***$P < .001$. Con, control adherent cells cultured in flask

the opposite effect (Figure S2C,D). Overexpression of c-Myc significantly promoted the TRC spheroid formation and growth of DAB2IP-overexpressing cells (Figure 3E,F). Furthermore, c-Myc overexpression largely rescued the DAB2IP-mediated inhibitory effect on Nanog, a well-known transcription factor for maintaining CSC self-renewal (Figures 3G and S2E). However, neither c-Myc overexpression nor knockdown modulated the expression of DAB2IP in HCT116 and HT29 cells (Figure S2F,G). Both IF staining and immunoblot analysis showed that TRC-derived xenograft tumors exhibited low expression of DAB2IP and high expression of c-Myc compared with that in the control group (Figures 3H,I and S2H). These results suggest that DAB2IP impairs TRC growth and self-renewal at least partially through negative regulation of c-Myc.

## 3.4 | DOC-2/DAB2 interactive protein promotes c-Myc protein degradation

To determine how DAB2IP downregulated c-Myc expression, we monitored mRNA levels by quantitative RT-PCR. Only a slight decrease of c-Myc mRNA levels was observed following DAB2IP transient overexpression (Figure 4A). As c-Myc was a highly unstable protein with a very short half-life,[22] we attempted to understand the post-translational regulatory mechanisms potentially involved to suppress c-Myc protein in DAB2IP-overexpressing cells. To determine whether DAB2IP modulated c-Myc protein stability, we treated cells with CHX, a de novo protein synthesis inhibitor. Accordingly, as the time of CHX

treatment was prolonged, DAB2IP transient overexpression significantly accelerated the turnover rate of c-Myc compared with control cells (Figure 4B). Furthermore, the proteasome inhibitor MG132 treatment largely blocked the DAB2IP-induced reduction of c-Myc protein, indicating that DAB2IP affected c-Myc protein stability (Figure 4C). Overexpression of DAB2IP enhanced ubiquitination of c-Myc in HCT116 and HT29 cells (Figure 4D). Given the key role of lysine(K) 48-linked polyubiquitination in c-Myc protein degradation,[23,24] we further determined weather DAB2IP orchestrated K48-linked ubiquitination of c-Myc. As shown in Figure 4E, overexpression of DAB2IP promoted endogenous K48-linked ubiquitination of c-Myc (Figure 4E). Collectively, these results suggest that DAB2IP disrupts c-Myc stability and enhances its ubiquitin-proteasome degradation.

## 3.5 | Glycogen synthase kinase 3β/protein phosphatase 2A-B56α-induced phosphorylation/dephosphorylation cascade contributes to DAB2IP modulation of c-Myc stability

Next, we intended to explore how DAB2IP regulated c-Myc stability. The degradation of c-Myc is largely dependent on an ordered GSK3β-mediated phosphorylation at threonine 58 (T58) site and subsequent protein phosphatase 2A (PP2A)-mediated dephosphorylation at serine 62 (S62) site.[25] Indeed, DAB2IP transient overexpression led to a reduction of S62 phosphorylation (p-c-Myc$^{S62}$) and an increase of T58 phosphorylation (p-c-Myc$^{T58}$) relative to total c-Myc protein in
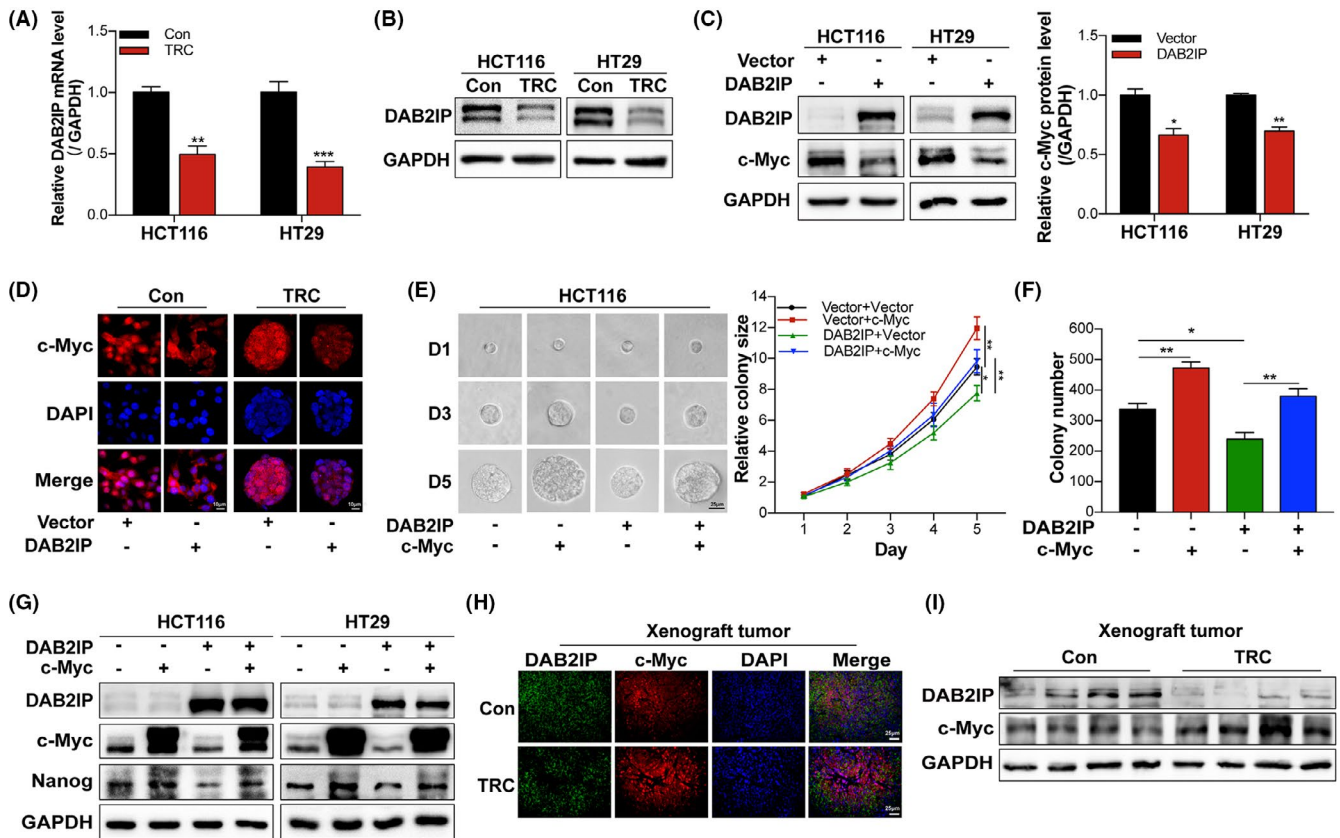
**FIGURE 3** DOC-2/DAB2 interactive protein (DAB2IP) downregulates c-Myc to suppress tumor-repopulating cell (TRC) growth and self-renewal. A, B, Quantitative RT-PCR (A) and immunoblot analysis (B) of DAB2IP expression in HCT116 and HT29 TRCs, vs their control cells. C, Immunoblot analysis of c-Myc levels in HCT116 and HT29 cells treated with vector or DAB2IP-overexpressing plasmids for 48 h. Relative c-Myc protein levels were quantitated using ImageJ software. D, Immunofluorescence (IF) staining of c-Myc levels in HCT116 cells treated with vector or DAB2IP-overexpressing plasmids. Scale bars, 10 μm. E, F, Impact of DAB2IP overexpression and/or c-Myc overexpression on TRC colony formation and growth. E, Left panel, Representative images of TRC spheroids. Scale bars, 25 μm. Right panel, Colony size calculated by ImageJ software. F, Colony numbers were counted at 96 h. G, Immunoblot analysis of Nanog expression in HCT116 and HT29 cells transfected with indicated plasmids. H, I, IF staining (H) and immunoblot analysis (I) of c-Myc and DAB2IP expression in xenograft tumor tissues derived from HCT116 TRCs or control cells. Scale bars, 25 μm. Data are shown as the mean ± SEM (n = 3). *P < .05, **P < .01, ***P < .001. Con, control adherent cells cultured in flask

HCT116 and HT29 cells (Figures 5A and S3A). The pS62 / pT58 ratio was significantly decreased, consistent with the decreased c-Myc stability (Figure 5A). We also found that colon TRCs showed increased S62 phosphorylation and decreased T58 phosphorylation relative to total c-Myc protein compared with control cells (Figure S3B). Of note, B56α (also known as PPP2R5A or PR61α), a key regulatory subunit of PP2A, directs the heterotrimeric PP2A complex to interact with dually phosphorylated c-Myc (T58/S62) and dephosphorylate c-Myc at S62 residue, which in turn triggers c-Myc ubiquitination and degradation.[26,27] We hypothesized that DAB2IP required B56α to promote S62 dephosphorylation of c-Myc. As anticipated, B56α silence rescued DAB2IP-induced downregulation of p-c-Myc$^{S62}$ (Figures 5B and S3C,D). Transiently overexpressed DAB2IP substantially strengthened the interaction between B56α and c-Myc without changing B56α expression (Figure 5C). Moreover, overexpression of DAB2IP downregulated serine 9 (S9) phosphorylation of GSK3β (p-GSK3β$^{S9}$, an inactive form of GSK3β), suggesting active GSK3β was increased (Figure 5D). Conversely, DAB2IP knockdown resulted in upregulation of p-GSK3β$^{S9}$

(Figure S3E). The GSK3β inhibitor LiCl largely reduced T58 phosphorylation and increased S62 phosphorylation in DAB2IP-overexpressing cells (Figures 5E and S3F), indicating that GSK3β activation was a prerequisite for DAB2IP to orchestrate c-Myc phosphorylation. Taken together, the above results demonstrate that DAB2IP modulates c-Myc stability through the GSK3β/PP2A-B56α-induced phosphorylation/dephosphorylation cascade.

Furthermore, given that DAB2IP is known as a scaffold protein that interacted with various proteins,[28-31] we wondered whether DAB2IP interacted with c-Myc. The IF staining showed that c-Myc was mainly located in the nucleus, and DAB2IP was localized both in the cytosol and nucleus under physiological conditions (Figure S3G). A coimmunoprecipitation analysis was undertaken and confirmed that endogenous DAB2IP interacted with endogenous c-Myc in HCT116 cells (Figure 5F). In addition, the DAB2IP-c-Myc interaction was confirmed following exogenous DAB2IP overexpression (Figure 5G). These results suggest that DAB2IP might also exert its function through interaction with c-Myc.
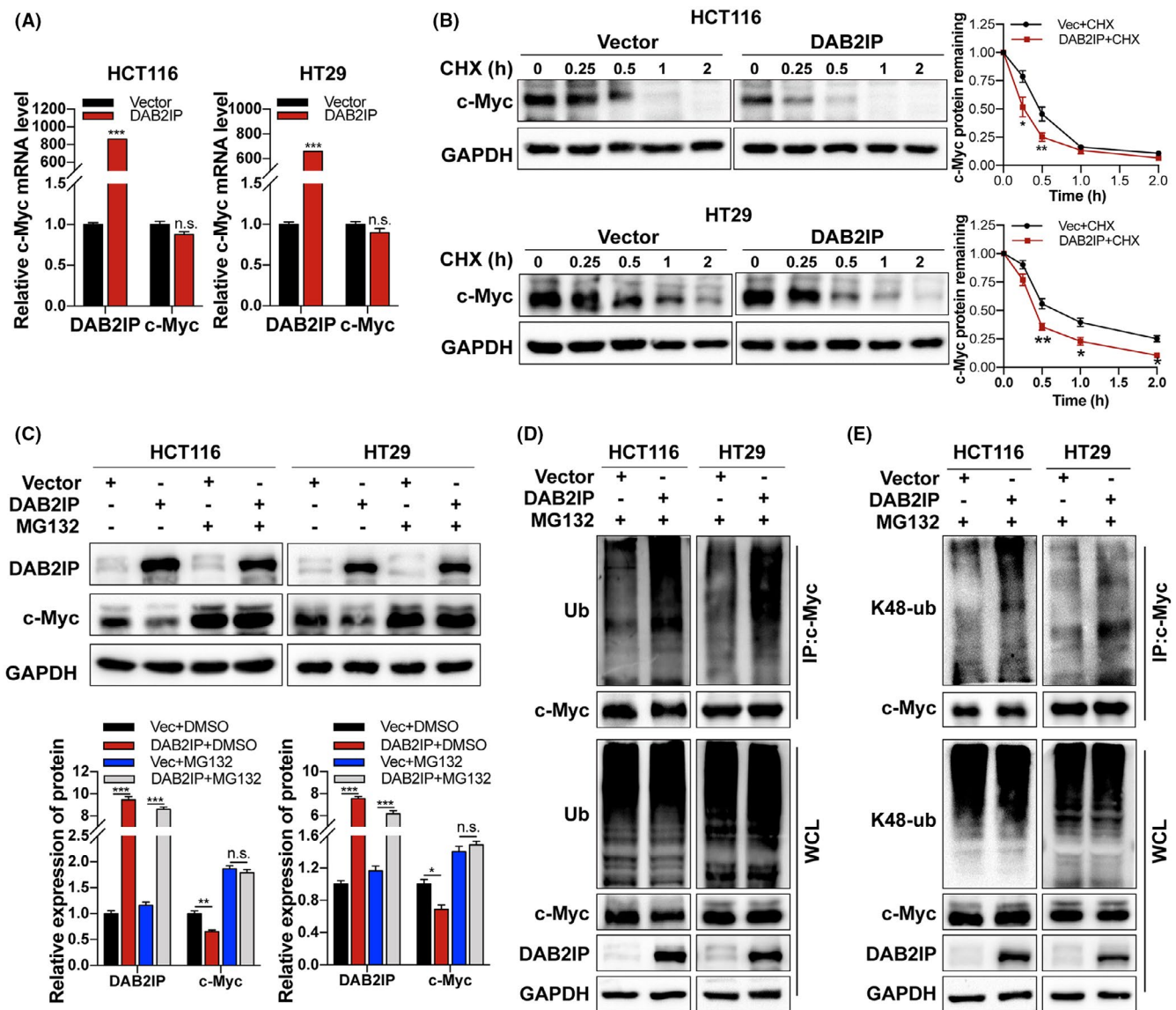
**FIGURE 4** DOC-2/DAB2 interactive protein (DAB2IP) decreases c-Myc stability and induces its degradation via ubiquitin-proteasome pathway. A, quantitative RT-PCR analysis of DAB2IP and c-Myc mRNA levels in HCT116 and HT29 cells transfected with indicated plasmids for 48 h. B, Immunoblot analysis of c-Myc expression in DAB2IP-overexpressing cells after treating with protein synthesis inhibitor cycloheximide (CHX, 100 μg/mL) in a time series. Right panels, Semiquantification of c-Myc levels, with GAPDH used as a loading control. C, Immunoblot analysis of c-Myc expression following DAB2IP transient overexpression after treating with MG132 (10 μmol/L, 6 h). Bottom left panel, Semiquantification of c-Myc levels, with GAPDH used as a loading control. D, Immunoblot analysis of ubiquitination of c-Myc in HCT116 and HT29 cells transfected with indicated plasmids. Cells were treated with MG132 for another 6 h and then subjected to immunoprecipitation (IP). E, Immunoblot analysis of specific endogenous K48-linked ubiquitination of c-Myc in HCT116 and HT29 cells transfected with indicated plasmids. Relative protein levels were quantitated using ImageJ software. Data are shown as the mean ± SEM (n = 3). *P < .05, **P < .01, ***P < .001. ns, not significant (P > .05). WCL, whole cell lysate. Ub, ubiquitin. K48-ub, K48-linked ubiquitin

## 3.6 | DOC-2/DAB2 interactive protein is negatively associated with c-Myc in CRC tissues and prognosis of CRC patients

We examined whether a correlation between DAB2IP and c-Myc expression existed in CRC tissues. As shown in Figure 6A, DAB2IP protein levels were downregulated and c-Myc was upregulated in tumor tissues compared with adjacent normal tissues (Figure 6A). Correlation analysis showed that DAB2IP expression was negatively

correlated with c-Myc (Figure 6B). The expression pattern of DAB2IP and c-Myc in CRC tissues was further confirmed by IHC (Figure 6C). The GSEA further indicated that low DAB2IP expression was significantly correlated with the MYC-activated target gene signature based on the GEO database (GSE39582 dataset; Figure 6D). In addition, low DAB2IP expression was significantly associated with distant metastasis in CRC patients from the GSE39582 dataset (Figure S4). Finally, we investigated the relationship between DAB2IP and the effectiveness of adjuvant treatment for CRC patients based on the
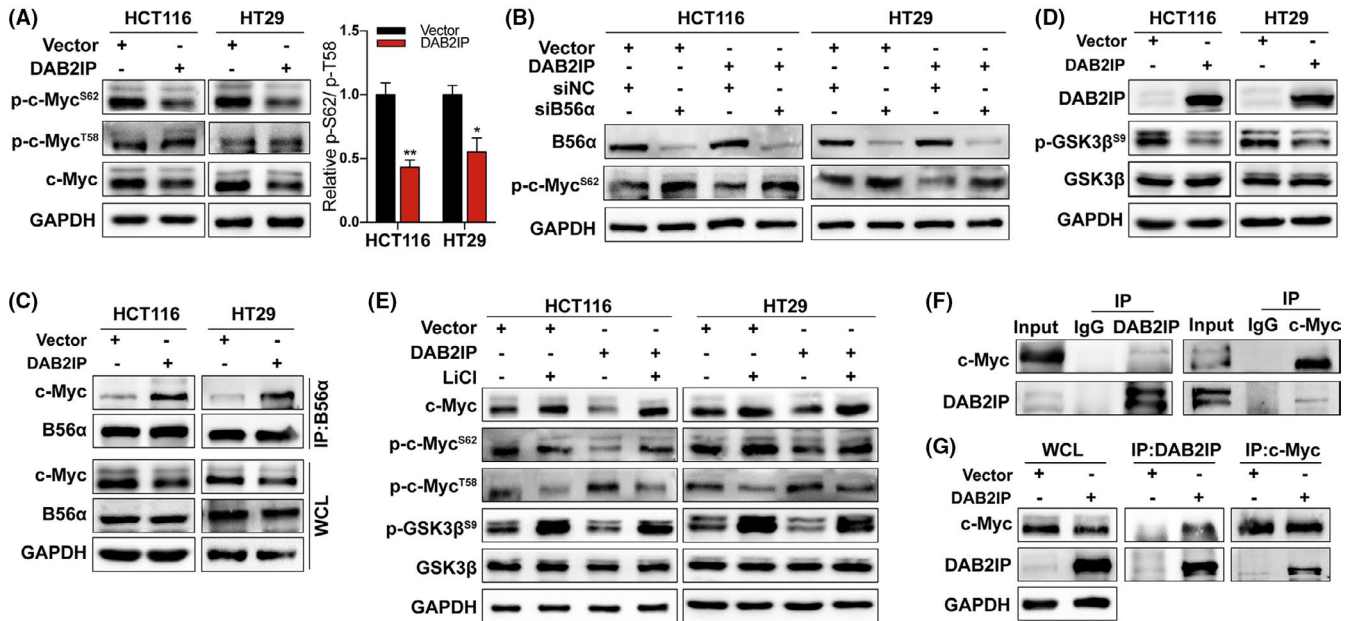
**FIGURE 5** DOC-2/DAB2 interactive protein (DAB2IP) destabilizes c-Myc through glycogen synthase kinase 3β (GSK3β)/protein phosphatase 2A (PP2A)-B56α-induced phosphorylation and dephosphorylation cascade. A, Immunoblot analysis of c-Myc, p-c-Myc$^{S62}$, and p-c-Myc$^{T58}$ levels in cells transfected with indicated plasmids. Relative protein levels were quantitated using ImageJ software. B, Immunoblot analysis of p-c-Myc$^{S62}$ levels in HCT116 and HT29 cells transfected with indicated plasmids and/or siRNA. C, Co-immunoprecipitation (Co-IP) assay was used to detect c-Myc-B56α interaction in cells transfected with indicated plasmids. D, Immunoblot analysis of GSK3β and p-GSK3β$^{S9}$ levels in HCT116 and HT29 cells transfected with indicated plasmids. E, Immunoblot analysis of p-GSK3β$^{S9}$, c-Myc, p-c-Myc$^{S62}$, and p-c-Myc$^{T58}$ levels in HCT116 and HT29 cells following GSK3β inhibitor LiCl (20 mmol/L, 6 h) treatment in the setting of DAB2IP overexpression. F, Co-IP assay was performed to detect endogenous interaction between DAB2IP and c-Myc in HCT116 cells. G, Co-IP assay was used to detect interaction between DAB2IP and c-Myc following DAB2IP overexpression in HCT116 cells. GAPDH was used as a loading control. Data are shown as the mean ± SEM (n = 3). *$P < .05$, **$P < .01$, ***$P < .001$. WCL, whole cell lysate

GSE103479 dataset. Colorectal cancer patients with low DAB2IP expression were not responsive to 5-fluorouracil-based adjuvant chemotherapy, whereas patients with high DAB2IP levels responded well and showed longer overall survival after adjuvant treatment (Figure 6E). These results indicate that DAB2IP expression is negatively associated with c-Myc in CRC tissues and could serve as a biomarker for tumor progression and response to therapy.

## 4 | DISCUSSION

The presence of tumorigenic and self-renewing CSC populations in CRC contributes to tumor recurrence and chemotherapy resistance.[32] Recent studies have revealed that TRCs truly exist as a highly malignant and tumorigenic subpopulation that are responsible for tumor initiation, metastasis, and treatment failure.[33,34] Thus, exploring the factors that regulate TRCs survival and self-renewal is an important step to identifying novel therapeutic targets. Several studies have linked the oncogenic transcription factor c-Myc to the self-renewal, proliferation, and tumorigenic potential of CSCs.[35] Because of its powerful roles in the transcription of numerous genes, even slight changes in c-Myc appear to have profound effects on the whole cellular environment.[36] Indeed, the expression of c-Myc is tightly regulated at transcriptional, posttranscriptional,

and posttranslational levels.[37-40] In the present study, the increased c-Myc protein expression with altered phosphorylation status was observed in colon TRCs compared with control cells. In addition, c-Myc knockdown reduced the number and size of TRC spheroids, suggesting that c-Myc was critical for TRC maintenance. The tumor suppressor DAB2IP, a Ras-GTPase activating protein with scaffolding function, is involved in various intracellular signaling pathways.[41-43] Here, we showed that DAB2IP promoted c-Myc degradation through the ubiquitin-proteasome pathway, which was linked to the exhaustion of colon TRC growth and self-renewal. The GSK3β/PP2A-B56α-mediated phosphorylation and dephosphorylation cascade on c-Myc protein contributed to DAB2IP modulation of c-Myc stability, leading to its eventual degradation. Moreover, our results expanded the scaffolding roles of DAB2IP to interact with c-Myc protein in HCT116 cells. Given the important roles of its scaffolding function, whether DAB2IP cooperates with other proteins to mediate distinct posttranslational modifications on c-Myc protein remains to be elucidated.

It is known that GSK3β also plays a critical role in regulating Wnt/β-catenin signaling.[44] Activated GSK3β is complexed with adenomatous polyposis coli (APC) and Axin to mediate β-catenin phosphorylation and degradation, resulting in the decreased transcription of its target gene *c-Myc*.[45] Previous studies reported that DAB2IP recruited PP2A to activate GSK3β, thus suppressing the
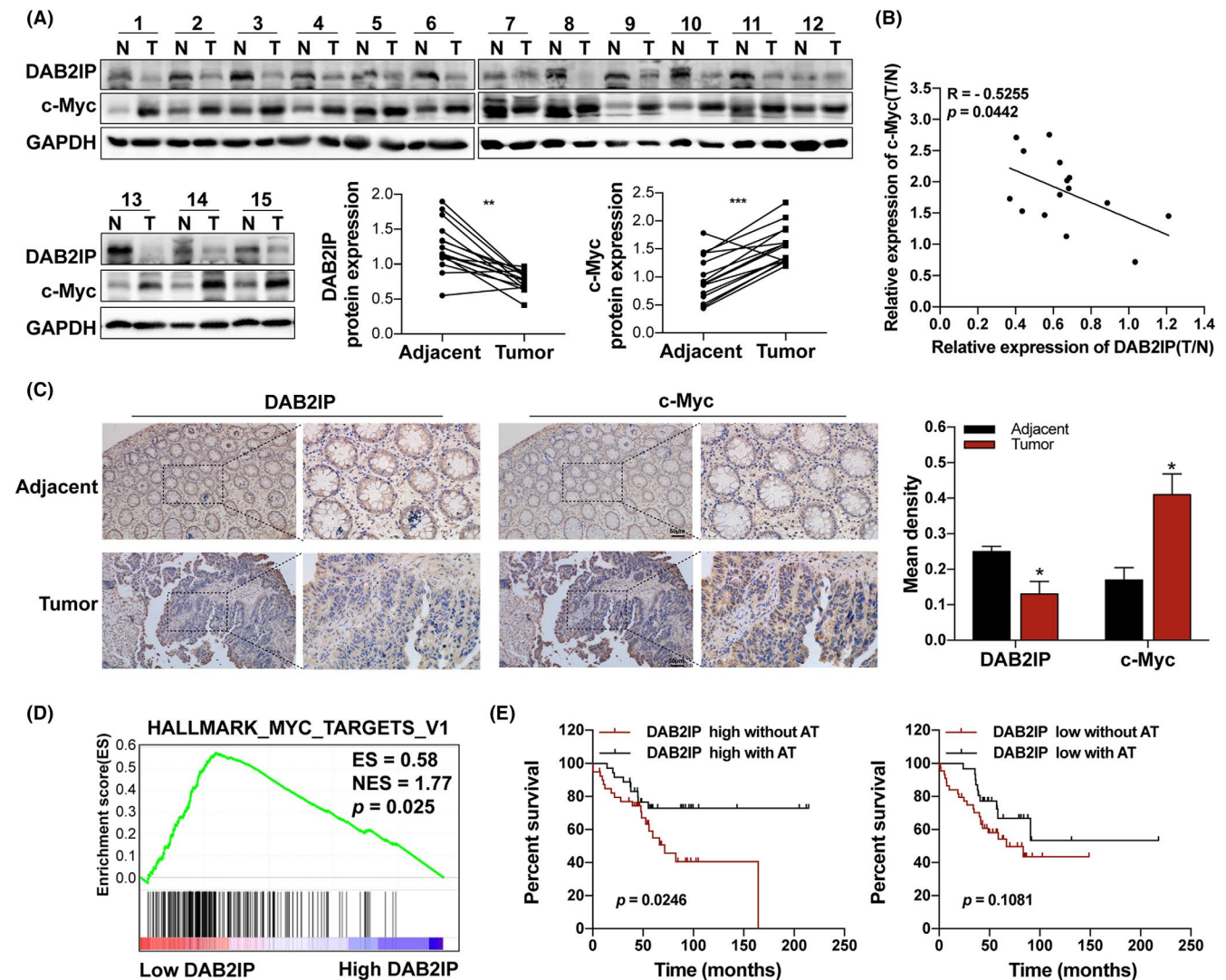
**FIGURE 6** DOC-2/DAB2 interactive protein (DAB2IP) is negatively associated with c-Myc in colorectal cancer (CRC) tissues. A, Immunoblot analysis of DAB2IP and c-Myc protein in 15 pairs of clinical CRC tissues (T) and corresponding adjacent normal samples (N). B, Relative DAB2IP and c-Myc expression was quantitated by ImageJ software, and their correlation was determined using Pearson's analysis. C, Left panels, Representative images of immunohistochemical staining for DAB2IP and c-Myc in CRC tissue samples. Scale bars, 50 μm. Right panel, Mean density was calculated by Image-Pro Plus 6.0. D, Correlation of DAB2IP expression and the MYC target signature in the GSE39582 dataset using Gene Set Enrichment Analysis (GSEA) (n = 566). ES, enrichment score; NES, normalized enrichment score. E, Kaplan-Meier survival curves of patients received with 5-fluorouracil-based adjuvant chemotherapy or not after surgery, classified by high (n = 76)/low (n = 76) DAB2IP expression in the GSE103479 dataset. GAPDH was used as a loading control. AT, adjuvant treatment. Data are shown as the mean ± SEM. *$P < .05$, **$P < .01$, ***$P < .001$ [Correction added on 5 November 2021, after first online publication: Figure 6E has been corrected and in its caption `high (n=78)/low (n=77)' was changed to `high (n = 76)/low (n = 76)'.]

Wnt/β-catenin pathway in prostate cancer and glioblastoma.[31,46] In this study, there was no obvious change in c-Myc mRNA levels following DAB2IP transient overexpression, which might be due to the different genetic backgrounds of cell lines and the complex regulatory mechanisms of c-Myc. The role of DAB2IP-mediated GSK3β activation in CRC was not universally identical due to the APC and β-catenin mutation status. It was reported that approximately 80% of CRC carried inactivating mutation in the APC gene or activating β-catenin mutation.[47,48] Both APC and β-catenin mutations contribute to constitutive stabilization of β-catenin and hyperactivation of Wnt/β-catenin signaling in human CRC.[49] Particularly, HT29 cells

bear APC mutation, and HCT116 cells harbor WT APC but serine 45 mutation in β-catenin, which prevents subsequent phosphorylation of β-catenin and its eventual degradation.[50,51] The APC or β-catenin mutation in those cells would result in less efficient GSK3β-mediated phosphorylation and degradation of β-catenin following DAB2IP overexpression. Consistently, Min et al reported that the β-catenin transcriptional activity was not changed in APC mutant SW480 cells following DAB2IP overexpression.[20] In addition, other DAB2IP-mediated signaling pathways might also be involved in transcriptionally regulating c-Myc in colon cancer cells, and the decreased c-Myc protein expression might activate an acute feedback mechanism to
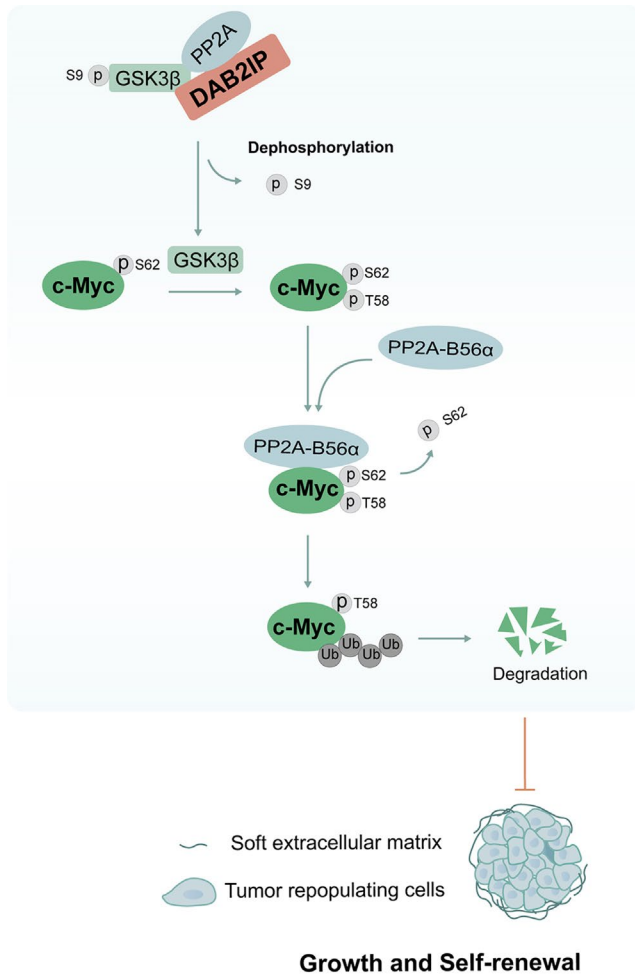
**FIGURE 7** Schematic representation of the role of DOC-2/DAB2 interactive protein (DAB2IP) in colon tumor-repopulating cells by regulating c-Myc stability. GSK3β, glycogen synthase kinase 3β; p, phosphorylation; PP2A, protein phosphatase 2A; Ub, ubiquitin

control its mRNA levels. Further investigations, in any case, are necessary for better understanding the complex regulatory network of c-Myc.

We provided evidence that DAB2IP expression was negatively correlated with c-Myc in CRC tissues. The DAB2IP expression was negatively associated with distant metastasis and the response to adjust chemotherapy treatment. We speculated that DAB2IP could be used as a diagnostic and prognostic biomarker of CRC. In conclusion, this study reveals that DAB2IP acts as a negative regulator to modulate c-Myc protein stability through the GSK3β/PP2A-B56α-dependent phosphorylation-dephosphorylation cascade, thus suppressing TRC growth and self-renewal (Figure 7).

**ORCID**

*Qiu Zhao* https://orcid.org/0000-0002-1596-5505
*Jing Liu* https://orcid.org/0000-0002-0958-5506

**REFERENCES**

1. Sung H, Ferlay J, Siegel RL, et al. Global cancer statistics 2020: GLOBOCAN estimates of incidence and mortality worldwide for 36 cancers in 185 countries. *CA Cancer J Clin*. 2021;71:209-249.
2. Biller LH, Schrag D. Diagnosis and treatment of metastatic colorectal cancer: a review. *JAMA*. 2021;325:669-685.
3. Akimoto N, Ugai T, Zhong R, et al. Rising incidence of early-onset colorectal cancer - a call to action. *Nat Rev Clin Oncol*. 2021;18:230-243.
4. Siegel RL, Miller KD, Goding Sauer A, et al. Colorectal cancer statistics, 2020. *CA Cancer J Clin*. 2020;70:145-164.
5. O'Connor ML, Xiang D, Shigdar S, et al. Cancer stem cells: a contentious hypothesis now moving forward. *Cancer Lett*. 2014;344:180-187.
6. Ricci-Vitiani L, Pagliuca A, Palio E, et al. Colon cancer stem cells. *Gut*. 2008;57:538-548.
7. Zeuner A, Todaro M, Stassi G, et al. Colorectal cancer stem cells: from the crypt to the clinic. *Cell Stem Cell*. 2014;15:692-705.
8. Zhang M, Xu C, Wang H-Z, et al. Soft fibrin matrix downregulates DAB2IP to promote Nanog-dependent growth of colon tumor-repopulating cells. *Cell Death Dis*. 2019;10:151.
9. Li Y, Song Y, Li P, et al. Downregulation of RIG-I mediated by ITGB3/c-SRC/STAT3 signaling confers resistance to interferon-α-induced apoptosis in tumor-repopulating cells of melanoma. *J Immunother Cancer*. 2020;8:e000111.
10. Liu J, Tan Y, Zhang H, et al. Soft fibrin gels promote selection and growth of tumorigenic cells. *Nat Mater*. 2012;11:734-741.
11. Ma J, Zhang YI, Tang KE, et al. Reversing drug resistance of soft tumor-repopulating cells by tumor cell-derived chemotherapeutic microparticles. *Cell Res*. 2016;26:713-727.
12. Cheung P, Xiol J, Dill MT, et al. Regenerative reprogramming of the intestinal stem cell state via hippo signaling suppresses metastatic colorectal cancer. *Cell Stem Cell*. 2020;27:590-604.e9.
13. Tan Y, Tajik A, Chen J, et al. Matrix softness regulates plasticity of tumour-repopulating cells via H3K9 demethylation and Sox2 expression. *Nat Commun*. 2014;5:4619.
14. Dang CV. MYC on the path to cancer. *Cell*. 2012;149:22-35.
15. Zhang H, Wang P, Lu M, et al. c-Myc maintains the self-renewal and chemoresistance properties of colon cancer stem cells. *Oncol Lett*. 2019;17:4487-4493.
16. Zhan W, Liao X, Wang Y, et al. circCTIC1 promotes the self-renewal of colon TICs through BPTF-dependent c-Myc expression. *Carcinogenesis*. 2019;40:560-568.
17. Bellazzo A, Di Minin G, Collavin L. Block one, unleash a hundred. Mechanisms of DAB2IP inactivation in cancer. *Cell Death Differ*. 2017;24:15-25.
18. Yun E-J, Lin C-J, Dang A, et al. Downregulation of human DAB2IP gene expression in renal cell carcinoma results in resistance to ionizing radiation. *Clin Cancer Res*. 2019;25:4542-4551.
19. Zong X, Wang W, Ozes A, et al. EZH2-mediated downregulation of the tumor suppressor DAB2IP maintains ovarian cancer stem cells. *Cancer Res*. 2020;80:4371-4385.

20. Min J, Liu L, Li X, et al. Absence of DAB2IP promotes cancer stem cell like signatures and indicates poor survival outcome in colorectal cancer. *Sci Rep*. 2015;5:16578.

21. Yun E-J, Baek ST, Xie D, et al. DAB2IP regulates cancer stem cell phenotypes through modulating stem cell factor receptor and ZEB1. *Oncogene*. 2015;34:2741-2752.

22. Welcker M, Orian A, Jin J, et al. The Fbw7 tumor suppressor regulates glycogen synthase kinase 3 phosphorylation-dependent c-Myc protein degradation. *Proc Natl Acad Sci USA*. 2004;15(101):9085-9090.

23. Farrell AS, Sears RC. MYC degradation. *Cold Spring Harb Perspect Med*. 2014;4:a014365.

24. Chandra S, Priyadarshini R, Madhavan V, et al. Enhancement of c-Myc degradation by BLM helicase leads to delayed tumor initiation. *J Cell Sci*. 2013;126:3782-3795.

25. Thomas LR, Tansey WP. Proteolytic control of the oncoprotein transcription factor Myc. *Adv Cancer Res*. 2011;110:77-106.

26. Sents W, Ivanova E, Lambrecht C, et al. The biogenesis of active protein phosphatase 2A holoenzymes: a tightly regulated process creating phosphatase specificity. *FEBS J*. 2013;280:644-661.

27. Arnold HK, Sears RC. Protein phosphatase 2A regulatory subunit B56alpha associates with c-myc and negatively regulates c-myc accumulation. *Mol Cell Biol*. 2006;26:2832-2844.

28. Yu L, Shang Z-F, Abdisalaam S, et al. Tumor suppressor protein DAB2IP participates in chromosomal stability maintenance through activating spindle assembly checkpoint and stabilizing kinetochore-microtubule attachments. *Nucleic Acids Res*. 2016;44:8842-8854.

29. Wu K, Liu J, Tseng S-F, et al. The role of DAB2IP in androgen receptor activation during prostate cancer progression. *Oncogene*. 2014;33:1954-1963.

30. Di Minin G, Bellazzo A, Dal Ferro M, et al. Mutant p53 reprograms TNF signaling in cancer cells through interaction with the tumor suppressor DAB2IP. *Mol Cell*. 2014;56:617-629.

31. Xie D, Gore C, Liu J, et al. Role of DAB2IP in modulating epithelial-to-mesenchymal transition and prostate cancer metastasis. *Proc Natl Acad Sci USA*. 2010;107:2485-2490.

32. Todaro M, Francipane MG, Medema JP, et al. Colon cancer stem cells: promise of targeted therapy. *Gastroenterology*. 2010;138:2151-2162.

33. Liu Y, Zhang T, Zhang H, et al. Cell softness prevents cytolytic T-cell killing of tumor-repopulating cells. *Cancer Res*. 2021;81:476-488.

34. Jiang M-J, Chen Y-Y, Dai J-J, et al. Dying tumor cell-derived exosomal miR-194-5p potentiates survival and repopulation of tumor repopulating cells upon radiotherapy in pancreatic cancer. *Mol Cancer*. 2020;19:68.

35. Das B, Pal B, Bhuyan R, et al. MYC regulates the HIF2α stemness pathway via Nanog and Sox2 to maintain self-renewal in cancer stem cells versus non-stem cancer cells. *Cancer Res*. 2019;79:4015-4025.

36. Duffy MJ, O'Grady S, Tang M, et al. MYC as a target for cancer treatment. *Cancer Treat Rev*. 2021;94:102154.

37. Uppada SB, Gowrikumar S, Ahmad R, et al. MASTL induces colon cancer progression and chemoresistance by promoting Wnt/β-catenin signaling. *Mol Cancer*. 2018;17:111.

38. Sheng X, Nenseth HZ, Qu SU, et al. IRE1α-XBP1s pathway promotes prostate cancer by activating c-MYC signaling. *Nat Commun*. 2019;10:323.

39. Jiang J, Wang J, Yue M, et al. Direct phosphorylation and stabilization of MYC by aurora B kinase promote T-cell leukemogenesis. *Cancer Cell*. 2020;37:200-215.

40. Fang X, Zhou W, Wu Q, et al. Deubiquitinase USP13 maintains glioblastoma stem cells by antagonizing FBXL14-mediated Myc ubiquitination. *J Exp Med*. 2017;214:245-267.

41. Min W, Lin Y, Tang S, et al. AIP1 recruits phosphatase PP2A to ASK1 in tumor necrosis factor-induced ASK1-JNK activation. *Circ Res*. 2008;102:840-848.

42. Xie D, Gore C, Zhou J, et al. DAB2IP coordinates both PI3K-Akt and ASK1 pathways for cell survival and apoptosis. *Proc Natl Acad Sci USA*. 2009;106:19878-19883.

43. Bellazzo A, Di Minin G, Valentino E, et al. Cell-autonomous and cell non-autonomous downregulation of tumor suppressor DAB2IP by microRNA-149-3p promotes aggressiveness of cancer cells. *Cell Death Differ*. 2018;25:1224-1238.

44. Nusse R, Clevers H. Wnt/β-catenin signaling, disease, and emerging therapeutic modalities. *Cell*. 2017;169:985-999.

45. van Andel H, Kocemba KA, Spaargaren M, et al. Aberrant Wnt signaling in multiple myeloma: molecular mechanisms and targeting options. *Leukemia*. 2019;33:1063-1075.

46. Yun E-J, Kim S, Hsieh J-T, et al. Wnt/β-catenin signaling pathway induces autophagy-mediated temozolomide-resistance in human glioblastoma. *Cell Death Dis*. 2020;11:771.

47. Fodde R, Smits R, Clevers H. APC, signal transduction and genetic instability in colorectal cancer. *Nat Rev Cancer*. 2001;1:55-67.

48. Network CGA. Comprehensive molecular characterization of human colon and rectal cancer. *Nature*. 2012;487:330-337.

49. Bugter JM, Fenderico N, Maurice MM. Mutations and mechanisms of WNT pathway tumour suppressors in cancer. *Nat Rev Cancer*. 2021;21:5-21.

50. Vijaya Chandra SH, Wacker I, Appelt UK, et al. A common role for various human truncated adenomatous polyposis coli isoforms in the control of beta-catenin activity and cell proliferation. *PLoS One*. 2012;7:e34479.

51. Ilyas M, Tomlinson IPM, Rowan A, et al. Beta-catenin mutations in cell lines established from human colorectal cancers. *Proc Natl Acad Sci USA*. 1997;94(19):10330-10334.

## SUPPORTING INFORMATION

Additional supporting information may be found online in the Supporting Information section.